




## ORIGINAL RESEARCH

# Managing reserve deliverability risk of integrated electricity-heat systems in day-ahead market: A distributionally robust joint chance constrained approach

Yang Chen<sup>1</sup> | Jianxue Wang<sup>1</sup>  | Siyuan Wang<sup>2</sup>  | Rui Bo<sup>3</sup> | Chenjia Gu<sup>1</sup>  | Qingtao Li<sup>1</sup>

<sup>1</sup>State Key Laboratory of Electrical Insulation and Power Equipment, School of Electrical Engineering, Xi'an Jiaotong University, Xi'an, China

<sup>2</sup>Whiting School of Engineering, Johns Hopkins University, Maryland, USA

<sup>3</sup>Department of Electrical and Computer Engineering, Missouri University of Science and Technology, Missouri, USA

## Correspondence

Jianxue Wang, State Key Laboratory of Electrical Insulation and Power Equipment, School of Electrical Engineering, Xi'an Jiaotong University, Xi'an, China.  
Email: jxwang@mail.xjtu.edu.cn

## Funding information

Natural Science Foundation of Jiangsu Province, Grant/Award Number: BK20222003

## Abstract

The integrated electricity and heat system (IEHS) is an emerging demand-side flexible resource for power systems. IEHS operators participating in electricity markets considering their capabilities in reserve provision will face the reserve deliverability risk due to the energy-limited storage nature of heat systems. To address this challenge and increase profitability, a distributionally robust joint chance-constrained mechanism with enhanced quantifications is adopted for the heating system and reserve deployment uncertainties. Detailed pipeline storage representation for thermal networks and integrated demand response are incorporated into this strategic participation model. A two-stage distributionally robust joint chance constrained program is then incorporated to effectively manage the reserve deliverability risk by addressing uncertainties from local distributed energy resources and real-time reserve requests. The L-shaped algorithm is then customized by incorporating bi-linear Benders' decomposition and modified scenario filtering method to efficiently tackle solution challenges for the sophisticated model. Numerical results show the advantages of our approach in virtual thermal storage utilization, risk management, computational performance enhancement and scalability.

## 1 | INTRODUCTION

The global transition towards a cleaner and carbon-neutral future is gaining momentum. Many countries are now taking bold steps towards a low-carbon future. In China, the closure of 13,729 MW of fuel-fired units by 2022 in the coal-dominated power system of Henan province exemplifies this shift [1]. The concept of multi-energy systems (MES) has emerged in the literature as a promising solution to future energy infrastructure [2]. MES are designed to integrate multiple energy carriers, including electricity, gas, and heat, to optimize resource utilization and increase energy efficiency. In urban energy systems, district heating (DH) is fundamental of providing hot water and space heating for domestic use, which are commonly seen in northern China and many European countries [3]. In recent years, the electrification and decarbonization process leads to

increasing availability of clean energy resources, such as gas-fired combined power and heat (CHP) units, electric boilers and heat pumps, which significantly enhance the flexibility of the combined system. This has led to the emergence of integrated electricity and heat systems (IEHS), which integrate DH networks (DHN) with power distribution networks (PDN) to optimize energy resource utilization, reduce operating costs, and facilitate the renewable energy resources (RES) accommodation [4]. Apart from efficient energy supplies to the local demands, the IEHS can provide ancillary services to benefit the grid [5]. Through the deregulation of the electricity markets, the IEHSs are able to aggregate local flexible resources to support the power systems via market participation so as to achieve higher profitability. Our motivation is to propose a comprehensive approach to derive the optimal bidding strategy of an IEHS in energy and reserve markets, which allows the IEHS operator

This is an open access article under the terms of the [Creative Commons Attribution](https://creativecommons.org/licenses/by/4.0/) License, which permits use, distribution and reproduction in any medium, provided the original work is properly cited.

© 2023 The Authors. *IET Generation, Transmission & Distribution* published by John Wiley & Sons Ltd on behalf of The Institution of Engineering and Technology.

to fully leverage the operational flexibility for optimal scheduling of the local DERs and loads as well as reserve provision to support the grid.

## 1.1 | Literature review

The optimal bidding strategy of the aggregators have been widely investigated [6]. A holistic approach is developed in [7] to derive the optimal offering strategy of a DER aggregator in the day-ahead markets. In [8], an optimal day-ahead market participation strategy is proposed for the local aggregators that integrates distributed generators, storage devices and demand response programs. As increasingly more distributed generation are embedded into the distribution networks, the traditional PDN are transitioning to the active distribution network (ADN) [9] that can proactively participate in energy markets. For instance, ref. [10] presents an optimal operation model considering the active managing costs of the source–network–load and the site selection and the incentive price for the responsive load. Further, a bi-level optimization model is proposed in [11] for the strategic participation of active distribution networks to provide energy and reserves in wholesale electricity markets.

The above works are contributed to optimal bidding strategies for electric facilities only. Nowadays, due to the high penetration of intermittent resources, the flexibility of stand-alone power system is usually limited. Integration of power system with other energy-carrier systems have been proposed to address this issue. Energy hub (EH) [12] presents a powerful MES management tool to balance multi-energy supplies and demands in the local area. Efforts are also underway to coordinate EHs in industrial parks and integrate them to participate in wholesale markets [13]. Considering the participation of distribution energy markets, the benefits of DER integration as an EH have been investigated in [14]. These works mainly focus on the integration of local energy resources, with the potential of energy networks themselves being underestimated.

The DHN consists of a large number of insulated pipelines that poses considerable amount of heat storage [15]. This inherent nature of DHN can be leveraged to provide ancillary services to the power systems. Recent years have seen an increasing interest in the reserve provision capability of the IEHS. Optimal energy and reserve models of the IEHS have been investigated in literature [16], with a focus on leveraging the flexibility in the DHN to cope with uncertainties in RES and provide multi-types of reserves. However, these works adopt a simplified thermal flow model that neglects the time delays of temperature changes along the pipelines. As a result, the potential of DHN flexibility cannot be fully accounted for.

Considering the energy-limited nature of the DHN, one significant concern is the reserve deliverability, which is defined in this paper as the ability to respond to the reserve deployment requests. As addressed in the literature, energy-limited resources including battery energy systems (BES) [17] and pumped storage systems (PSH) [18] usually face the risk of state-of-charge (SOC) violation due to sustained unidirectional reserve requests over time. Neglecting the energy-limited nature often result in

over-optimistic solutions. Similar to these facilities, the SOC of the DHN can be implicitly represented by the energy stored in the hot water circling in the pipelines. IEHS operators, as flexibility providers, must manage the risk associated with reserve deliverability under various sources of uncertainty. Some relevant works have addressed similar concerns. For example, in [19], the energy storage of smart buildings in the IEHS is modelled to provide additional flexibility to provide reserves. In this work, robust reserve provision constraints are proposed with a very strong guarantee of reserve deliverability under all possible occasions. However, this approach may result in over-conservative results since the requested reserve capacity is unlikely to be constant throughout the system's operation. Therefore, powerful risk management techniques are crucial for addressing the reserve deliverability issue while avoiding over-optimistic or over-conservative outcomes.

A set of mathematical tools have been adopted to manage the diverse uncertainties in a market environment. Stochastic programming (SP) is commonly seen in the literature related to strategic market participation as a risk management tool against uncertainties [11, 20]. In these works, the decision maker only cares about the potential or expected gains while neglects the downside risks. Robust optimization (RO) [21] is also frequently used to handle the uncertainties, which provides conservative solutions considering all uncertainty realizations. Chance constrained programming (CCP) is another group of risk management method, in which decision makers focus on ensuring certain constraints are satisfied with a confident level. In [22], a CCP model is proposed for strategic bidding of a micro-grid embedded EH, where chance constraints are introduced to relax the thermal supply requirements in extreme cases. Note that the conditional value-at-risk method (CVaR) is sometimes considered as a specific formulation of CCP that preserves convexity [23]. For example, a CVaR-based stochastic scheduling of MES is proposed in [24] integrating the uncertainty of wind power generation. Besides, using information-gap decision theory (IGDT) techniques, both risk-averse and risk-seeking bidding strategy can be proposed for an EH operator [25].

Distributionally robust optimization (DRO) [26] have been developed in recent years as an intermediate method between SP and RO that considers the uncertainties under the worst probability distribution, which is regarded as a practical data-driven approach that can fully leverage the historic data for the guess of suitable distribution. Further, the distributionally robust chance constrained programming make a combination of traditional CCP and DRO method by introducing the DR ambiguity set into the chance constraints, providing a risk-averse extension of CCP that improves the robustness of the solution, as recently adopted in [27] for reserve provision problem of the ADN. The application of distributionally robust chance constrained programming provides the IEHS operators an effective risk management tool.

Aforementioned works based on DRO models usually assume a linear or affine policies to the recourse problem for tractability [27, 28]. This simplification, however, limits the flexibility in recourse problems and could also be time-consuming with high-dimensional variables. Alternatively, decomposition

methods, such as the L-shaped algorithm, are used to iteratively solve these models. In [29], a distributionally robust L-shaped algorithm is proposed to solve two-stage DRO models, with a finite-step convergence proof with moment or Wasserstein metric based confident set. Extended to distributionally robust chance constrained programming, ref. [30] proposes a general mixed integer reformulation for the DR individual and joint chance constraints. However, computational efficiency is still a challenge when considering large number of scenarios.

## 1.2 | Research gaps

Although great efforts have been made, there are still noteworthy deficiencies in the current works:

1. Despite the considerable research that has been carried out on employing DHN as a virtual energy storage system to enhance power system flexibility, efforts on exploring reserve provision capability of the IEHS are still limited. Existing studies predominantly rely on simplified thermal flow models, which may underestimate the true impact of the DHN and potentially hinder the profitability of IEHS.
2. While the topic of reserve deliverability risk has been widely studied for traditional energy-limited resources such as BES systems and PSH units, the relevant literature regarding the IEHS, which represents a novel type of energy-limited resource, remains scant. To enable more effective participation in electricity markets, it is essential to develop appropriate risk management tools for the IEHS that can account for multi-source of uncertainty, especially the reserve deliverability risk, to avoid over-optimistic or over-conservative results.
3. Though both CCP and DRO approaches possess many desirable characteristics as popular used risk management tools, their combination presents a considerable computational obstacle and limits their application to MES operation. Efficient algorithms should be proposed to address this issue.

## 1.3 | Contributions and paper organization

Here, we present a two-stage distributionally robust joint chance constrained program (DRJCCP) for risk-averse bidding strategy of the IEHS in ISO day-ahead energy and reserve markets. The schematic graph of the IEHS can be depicted in Figure 1. The main contributions of this paper are threefold:

1. An optimal market participation model of the IEHS is developed considering the provision of reserves to the upper-level power system. By incorporating detailed thermal flow modelling and integrated demand response from smart buildings, the DHN is modelled as a new type of energy-limited resource that can be utilized to hedge against multi-source uncertainties. We show this modelling can dramatically enhance the operational flexibility of the IEHS.

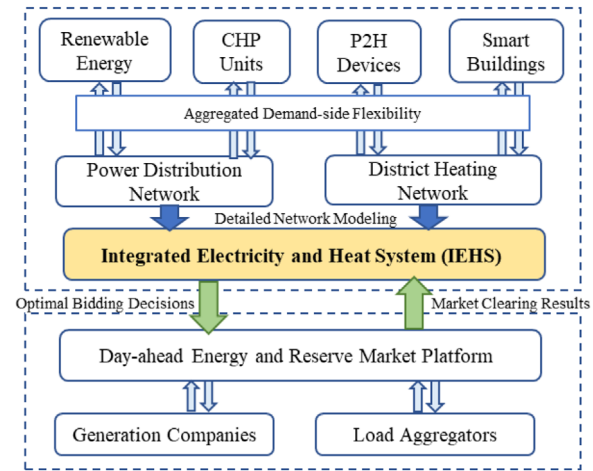


**FIGURE 1** The scheme of the integrated electricity and heat system (IEHS) studied in this paper.

2. A novel DRJCC formulation is proposed to account for the uncertainties associated with local RES and real-time reserve deployment. This model offers reliable and less conservative solution of the bidding strategy for the IEHS. In addition, the joint chance constrained mechanism is introduced to reconstruct temperature-related constraints of the DHN to provide extra operational flexibility, which enables the IEHS operator to supply “low-quality” thermal energy in extreme scenarios to avoid deviations from reserve requests.
3. An efficient solving procedure is developed to address the computational challenge with the DRJCCP. Specifically, the bilinear variant of Benders’ decomposition is applied to customize the traditional L-shaped algorithm to efficiently solve the proposed model with mixed integer constraints. Additionally, a heuristic scenario filtering method is proposed to achieve fast computation.

The rest of the paper is organized as follows. Section 2 introduces the strategic market participation model of the IEHS. In Sections 3, the revised L-shaped algorithm and the solution method for the proposed model is introduced. Section 4 shows and discusses the test results on two test systems. Section 5 makes a conclusion.

## 2 | OPTIMAL BIDDING STRATEGY OF THE RISK-AVERSE IEHS OPERATOR

### 2.1 | Upper-level: Optimal operation of the IEHS

In the upper-level problem, the IEHS optimize the bidding strategy in participating the energy and reserve markets based on the equipped DERs and the power-heat network coordination. The IEHS operator can strategically change the offered prices and the bid quantities for energy and operating reserves to maximize its total profit.

### 2.1.1 | Objective function

The objective function of the operator is to gain more profit from the markets and minimize the expected operating costs of the IEHS.

$$\min C^{E\&RM} + C^{RT,C} + C^{RT,M} \quad (1a)$$

$$C^{E\&RM} = - \sum_{t \in T} \left( -\lambda_{t,s}^E P_t^{EH} + \lambda_t^{R,U} R_t^{EH,U} + \lambda_t^{R,D} R_t^{EH,D} \right) \quad (1b)$$

$$C^{RT,C} = \sum_s \pi_s \sum_{t \in T} \left( \sum_{g \in \mathcal{G}^{CHP}} \left( c_{g,t,s}^{CHP,E} p_{g,t,s}^{CHP} + c_{g,t,s}^{CHP,H} p_{g,t,s}^{CHP} \right) + \sum_{g \in \mathcal{G}^{PV}} c_{g,t,s}^{PV,E} p_{g,t,s}^{PV} \right) \quad (1c)$$

$$C^{RT,M} = \sum_s \pi_s \sum_{t \in T} \left( -\bar{\lambda}_{t,s}^E P_{t,s}^{PCC,D} + \lambda_t^{pen} P_{t,s}^{mis} \right) \quad (1d)$$

where the objective consists of three parts: the cost (reverse revenue) from the day-ahead market (1b), the real-time operating costs for the DERs (1c) and real-time market settlement (1d).

### 2.1.2 | Constraints for reserve provision and deployment

Then, as shown in (2a),  $P_{t,s}^{PCC}$  and  $P_{t,s}^{PCC,D}$  are introduced to describe the real-time power exchange and the deviation from the day-ahead committed quantity  $P_{t,t}^{EH}$  in scenario  $s$  at time  $t$ , respectively. Note that the real-time deviation is driven by two main factors. One is the real time reserve deployment from the ISO, while the other comes from the output variety from the local intermittent RES, which is modelled in the PDN constraints.

Once the IEHS sells reserve commitment in the day-ahead market, it is obliged to follow the request from ISO. In the real time stage, the request of reserve deployment from the ISO can be represented as the portion of the committed reserve capacity in the ISO market, as shown in (2b). If not satisfied, the mismatched amount will be charged at an uninstructed deviation penalty price [31]. To model the uncertainty of systematic reserve deployment, random parameters  $(\alpha_{t,s}^{R,U}, \alpha_{t,s}^{R,D})$  are introduced to represent the deployed ratio for upward/downward reserve in scenario  $s$  at time  $t$ . In this model,  $P_{t,s}^{mis}$  is introduced to describe the mismatch from the system reserve request (2c). Equation (2d) is a deliverability requirement constraint to ensure that the total mismatch mileage during a day should not exceed a certain level restricted by the ratio of maximal deviation  $\delta$ .

$$P_{t,s}^{PCC} = P_{t,t}^{EH} + P_{t,s}^{PCC,D}, \quad \forall t, s \quad (2a)$$

$$r_{t,s}^R = \alpha_{t,s}^{R,U} R_t^{EH,U} - \alpha_{t,s}^{R,D} R_t^{EH,D}, \quad \forall t, s \quad (2b)$$

$$P_{t,s}^{mis} \geq \left| r_{t,s}^R - P_{t,s}^{PCC,D} \right|, \quad \forall t, s \quad (2c)$$

$$0 \leq \sum_t P_{t,s}^{mis} \leq \delta \sum_t \left( R_t^{EH,U} + R_t^{EH,D} \right) \Delta T, \quad \forall s \quad (2d)$$

### 2.1.3 | PDN side constraints

The linear distribution power flow [32] is adapted to model the active/reactive power flow in the power distribution system, as shown in (3). Equations (3a)–(3c) are active/reactive power generation constraints and ramping constraints for thermal units. Equation (3d) defines the power exchange at the PCC node to be the sum of the branch flows starting from the root node. Equations (3e), (3f) represent the nodal balance constraints of active and reactive power at each bus. Equations (3g), (3h) represent the constraints for the voltage magnitude.

$$P_{-g}^k u_{g,t} \leq p_{g,t,s}^k \leq \bar{P}_g^k u_{g,t}, -\beta p_{g,t,s}^k \leq q_{g,t,s}^k \leq \beta p_{g,t,s}^k, \quad \forall g \in \mathcal{G}^k, \quad k = \{CHP, TU\}, t, s \quad (3a)$$

$$p_{g,t,s}^k - p_{g,t-1,s}^k \leq RU_g, \quad \forall g \in \mathcal{G}^k, k = \{CHP, TU\}, t, s \quad (3b)$$

$$p_{g,t-1,s}^k - p_{g,t,s}^k \leq RD_g, \quad \forall g \in \mathcal{G}^k, k = \{CHP, TU\}, t, s \quad (3c)$$

$$P_{t,s}^{PCC} = \sum_{b \in N_1^{cb}} P_{b,t,s}, \quad \forall t, s \quad (3d)$$

$$\sum_{g \in \mathcal{G}_n^{CHP}} p_{g,t,s}^{CHP} + \sum_{g \in \mathcal{G}_n^{EB}} p_{g,t,s} + \sum_{g \in \mathcal{G}_n^{PV}} p_{g,t,s}^{PV} + P_{mn,t,s} = \sum_{b \in N_n^{cb}} P_{b,t,s} + p_{n,t,s}^D, \quad \forall n \in N^E, t, s \quad (3e)$$

$$\sum_{g \in \mathcal{G}_n^{CHP}} q_{g,t,s} + Q_{mn,t,s} = \sum_{b \in N_n^{cb}} Q_{b,t,s} + q_{n,t,s}^D, \quad \forall n, t, s \quad (3f)$$

$$v_{n,t,s} = v_{m,t,s} - \frac{r_{mn} P_{mn,t,s} + x_{mn} Q_{mn,t,s}}{v_0}, \quad \forall m, n \in N_m^{cb}, t, s \quad (3g)$$

$$V_- \leq v_{n,t,s} \leq \bar{V}, \quad \forall n, t, s \quad (3h)$$

### 2.1.4 | DHN side constraints with pipeline storage modelling

For the district heating network, the pipelines are modelled in detail using node method [15]. The DHN contains multiple source nodes and multiple load and immediate nodes, which are connected by pipelines. Commonly, the thermal energy is transmitted from source nodes to the load nodes through the



supply network. After serving the loads, the water is cooled down and flows back via the return network and complete the circulation [33]. The DHN-related constraints are presented in (4). In (4a), the thermal power generation comes from the CHP units and power-to-heat (P2H) devices like electric boilers (EB). For each generator  $g$ , the relation of electric power and thermal power can be uniformly described by the P2H ratio  $\eta_g^{P2H}$ . The relation of thermal power injection and abstraction with the mass flow rate and temperature change can be calculated according to (4b) and (4c).

$$b_{g,t,s}^k = \eta_g^{P2H} p_{g,t,s}^k, \forall g \in \mathcal{G}^k, k = \{CHP, EB\}, t, s \quad (4a)$$

$$\sum_{g \in \mathcal{G}_i^{CHP}} b_{g,t,s}^{CHP} + \sum_{g \in \mathcal{G}_i^{EB}} b_{g,t,s}^{EB} = c_w m_{i,t}^G (\tau_{i,t,s}^{GS} - \tau_{i,t,s}^{GR}), \forall i \in N^{HS}, t, s \quad (4b)$$

$$b_{i,t,s}^D = -c_w m_{i,t}^D (\tau_{i,t,s}^{DS} - \tau_{i,t,s}^{DR}), \forall i \in N^{HD}, t, s \quad (4c)$$

In this section, the relationship of the inlet and outlet temperature  $\tau_{ij,t,\omega}^{S,out}$  and  $\tau_{ij,t,\omega}^{S,in}$  of the pipelines can be written in (5), which are elaborated in [15].  $K_{ij,t,k}$  denotes the heat transfer delay coefficient for pipeline  $ij$  indicating the impact of inlet temperature at time  $k$  on the outlet temperature at time  $t$ .  $J_{ij,t}$  represents the heat loss coefficient along the pipeline  $ij$ .  $\hat{\tau}_{ij,t}^{S,out}$  and  $\hat{\tau}_{ij,t}^{R,out}$  are constants related to historical temperature profiles.  $\tau_{ij,t,\omega}^{S/R,out*}$  denotes the equivalent outlet temperature of pipeline  $ij$ .

$$\tau_{ij,t,s}^{S/R,out*} = \sum_{k=1}^t K_{ij,t,k} \tau_{ij,k,s}^{S/R,in} + \hat{\tau}_{ij,t}^{S/R,out}, \forall j \in N_i^{S/R(+)}, t \quad (5a)$$

$$\tau_{ij,t,s}^{S/R,out} = \hat{\tau}_t^{AM} + J_{ij,t} (\tau_{ij,t,s}^{S/R,out*} - \hat{\tau}_t^{AM}), \forall j \in N_i^{S/R(+)}, t \quad (5b)$$

In (6), the thermal flow equations are presented. Equations (6a) and (6b) model the nodal temperature mixing process. According to the first law of thermodynamics, the nodal temperature can be calculated by the inlet temperature weighted by the related mass flow rate. Besides, as shown in (6c), the inlet temperature of the pipelines starting from this node is equal to the nodal temperature. And in (6d), the temperature of the load at the supply end and that of the source at the return end should be equal to the related nodal temperature. Last but not least, (6e) restricts the temporal variables by upper and lower bounds.

$$\sum_i (\hat{m}_{ij,t} \tau_{ij,t,s}^{S,out}) + \hat{m}_{j,t}^G \tau_{j,t,s}^{GS} = \left( \sum_i \hat{m}_{ij,t} + \hat{m}_{i,t}^G \right) \tau_{j,t,s}^{NS}, \forall j, t, s \quad (6a)$$

$$\sum_i (\hat{m}_{ij,t} \tau_{ij,t,s}^{R,out}) + \tau_{j,t,s}^{DR} \hat{m}_{j,t}^D = \left( \sum_i \hat{m}_{ij,t} + \hat{m}_{i,t}^D \right) \tau_{j,t,s}^{NR}, \forall j, t, s \quad (6b)$$

$$\tau_{ij,t,s}^{S,in} = \tau_{i,t,s}^{NS}, \tau_{ij,t,s}^{R,in} = \tau_{j,t,s}^{NR}, \forall i, j, t, s \quad (6c)$$

$$\tau_{j,t,s}^{DS} = \tau_{j,t,s}^{NS}, \tau_{j,t,s}^{GR} = \tau_{j,t,s}^{NR}, \forall j, t, s \quad (6d)$$

$$\tau_{-}^{NS} \leq \tau_{j,t,s}^{NS} \leq \bar{\tau}^{NS}, \tau_{-}^{NR} \leq \tau_{j,t,s}^{NR} \leq \bar{\tau}^{NR}, \forall j, t, s \quad (6e)$$

By applying this detailed thermal network model with pipeline storage, the thermal transmission delays can be addressed so that the DHN can be treated as a virtual energy storage.

### 2.1.5 | Integrated demand response constraints

Smart buildings have been regarded as new flexible load resources and widely studied as in [19, 34]. As an end-user connected to both PDN and DHN, the heat demand in smart buildings can be satisfied by the heat supplies directly from the DHN or by domestic power-to-heat devices such as space heaters, air conditioners etc. To maintain the indoor temperature of a building, a certain amount of thermal energy should be consumed by the end-user. The total heat injected to the building at node  $n$  consists of the heat transfer from the DHN and the domestic P2H devices. Then, the integrated demand response can be modelled as in (7). Equation (7a) describes the temperature dynamics of the end-user at node  $n$ . Equation (7b) models the upper and lower bounds for the indoor temperature. And (7c), (7e) model the heat reschedules of the end-users, where  $p_{n,t,s}^D$  and  $b_{i,t,s}^D$  denote the net power and heat consumed via the networks.

$$\eta^H b_{i,t,s}^D + U_i (\hat{\tau}_t^{AM} - \tau_{i,t,s}^{IN}) = \tau_{i,t,s}^{IN} - \tau_{i,t-1,s}^{IN}, \forall i, t, s \quad (7a)$$

$$\tau_{-i}^{IN} \leq \tau_{i,t,s}^{IN} \leq \bar{\tau}_i^{IN}, \forall i, t \quad (7b)$$

$$p_{n,t,s}^D = \hat{p}_{n,t,s}^D + p_{n,t,s}^{DH}, \forall n \in \Xi(i), t, s \quad (7c)$$

$$b_{i,t,s}^D = \hat{b}_{i,t,s}^D - b_{n,t,s}^{DH}, \forall i, t, s \quad (7d)$$

$$0 \leq p_{n,t,s}^{DH} \leq \bar{p}_n^{DH}, b_{n,t,s}^{DH} = \eta^{DH} p_{n,t,s}^{DH}, \forall n \in \Xi(i), t, s \quad (7e)$$

### 2.1.6 | Bidding constraints

For an IEHS located at bus  $l$  in transmission system, the price bids for energy and reserve should be bounded according to the system requirements.

$$0 \leq o_{l,t}^{EH,E} \leq \bar{o}_l^E, 0 \leq o_{l,t}^{EH,RU/RD} \leq \bar{o}_l^{RU/RD}, \forall t \quad (8)$$

## 2.2 | Lower-level: Energy-reserve market clearing

In the lower level, the ISO performs the market clearing process after receiving bids and offers from market participants to maximize the total social welfare. In this ISO day-ahead market, the energy and operating reserve are joint cleared for each hour. Thus, the objective (9a) is to minimize the total operating costs.  $\bar{p}_{l,t}^{IES}$  denotes the net injection of the IEHS  $l$  at the PCC node. Equation (9b) presents the line constraints for the power transmission system. Equation (9c) denotes the constraints to meet the total upward/downward reserve requirements of the ISO. Equation (9d) represents the power balance constraints. Equations (9e), (9h) are bounding constraints for the market participants including the IEHS and traditional generation companies. Equation (9i) is the ramping constraints for generators.

$$\min \sum_f \left( \sum_f o_{f,t}^{GC,E} \bar{p}_{f,t}^{GC} + o_{f,t}^{GC,RU} R_{f,t}^{GC,U} + o_{f,t}^{RD} R_{f,t}^{GC,D} \right) - \left( o_{l,t}^{EH,E} \bar{p}_{l,t}^{EH} + o_{l,t}^{EH,RU} R_{l,t}^U + o_{l,t}^{EH,RD} R_{l,t}^D \right), \forall t \quad (9a)$$

$$-\bar{P}_{fl} \leq \sum_{l'} PIDF_{fl,l'} \left( -\bar{p}_{l',t}^D + \bar{p}_{l',t}^{GC} - \sum_k \bar{p}_{l',t}^{EH} \right) \leq \bar{P}_{fl} : \mu_{fl,t}^\pm \quad (9b)$$

$$R_t^{Sys,U/D} = \sum_f R_{f,t}^{GC,U/D} + R_{l,t}^{EH,U/D} : \lambda_t^{R,U/D} \quad (9c)$$

$$\sum_l \left( -\bar{p}_{l,t}^{EH} - \bar{p}_{l,t}^D + \bar{p}_{l,t}^{GC} \right) = 0 : \lambda_t^E \quad (9d)$$

$$\bar{p}_{-l}^{GC} + R_{l,t}^{GC,D} \leq \bar{p}_{l,t}^{GC} \leq \bar{p}_l^{GC} - R_{l,t}^{GC,U} : \mu_{l,t}^{GC,CAP\pm} \quad (9e)$$

$$\bar{p}_{-l}^{EH} + R_{l,t}^{EH,U} \leq \bar{p}_{l,t}^{EH} \leq \bar{p}_l^{EH} - R_{l,t}^{EH,D} : \mu_{l,t}^{EH,CAP\pm} \quad (9f)$$

$$0 \leq \bar{p}_{l,t}^{GC/EH} \leq \bar{p}_{l,t}^{GC/EH,Bid} : \mu_{l,t}^{GC/EH\pm} \quad (9g)$$

$$0 \leq R_{l,t}^{GC/EH,U/D} \leq R_{l,t}^{GC/EH,U/D,Bid} : \mu_{l,t}^{U/D\pm} \quad (9h)$$

$$-R_{l,t}^{RP} \leq \bar{p}_{l,t}^{GC} - \bar{p}_{l,t-1}^{GC} \leq R_{l,t}^{RP} : \mu_{l,t}^{RP\pm} \quad (9i)$$

## 2.3 | Risk-averse bidding strategy

In practice, the market participants tend to become risk-averse decision makers. In this case, a risk-averse strategy seeks for the worst distribution  $\mathbf{P}^*$  that maximizes the operating costs. Then, real-time cost  $C^{RT,C}$  in (1c) can be rewritten as in (10).

$$C^{RT,C} = \max_{\mathbf{P} \in \mathbb{D}} \sum_s \pi_s \sum_{t \in T} \left( \sum_{g \in \mathcal{G}^{CHP}} (c_{g,t,s}^{CHP,E} \bar{p}_{g,t,s}^{CHP} + c_{g,t,s}^{CHP,H} \bar{b}_{g,t,s}^{CHP}) + \sum_{g \in \mathcal{G}^{PV}} c_{g,t,s}^{PV,E} \bar{p}_{g,t,s}^{PV} \right) \quad (10)$$

In (10), the probability distribution of the random variables in this model is assumed to be unknown and can vary within the confident set  $\mathbb{D}$ . And then, the Wasserstein metric is used in this work to construct the confidence set with empirical data of the local RES outputs as well as the reserve request from ISO in the real time. We can model the confidence set  $\mathbb{D}$  in (11).

$$\sum_{s=1}^N \sum_{s'=1}^N \pi_{ss'} \delta_{ss'} \leq \theta \quad (11a)$$

$$\sum_{s'=1}^N \pi_{ss'} = \pi_s \quad (11b)$$

$$\sum_{s=1}^N \pi_{ss'} = \hat{\pi}_{s'} \quad (11c)$$

$$\sum_{s'=1}^N \pi_{s'} = 1 \quad (11d)$$

where  $\pi_s$  and  $\hat{\pi}_s$  are the true and empirical distribution probability of scenario  $s$ , respectively.  $\theta$  present the tolerance of Wasserstein distance that can be determined by a given confidence level  $\alpha$ , the number of bins  $N$ , the diameter of supporting space  $\delta$ , and the size of historical data  $N_b$ , as depicted in [26].

Applying the detailed thermal flow model in (6) and the demand model in (7), the thermal energy supply is guaranteed in all occasions. However, unlike the power systems that apply rather strict technique limitations on voltage and current to ensure the security of operation, the limitations on temperature for the heat systems can be treated as soft constraints. Violation of these constraints usually degrades the quality of thermal supply. In some extreme scenarios, the quality of thermal supply can be flexible. In other words, the operator can choose to provide low-quality heat in some cases to eliminate the deviations from reserve requests. To address this, DRJCC of the temperature-related constraints are then introduced to eliminate non-responsive scenarios under a given confidence level  $\varepsilon$ . These constraints can be violated in some extreme conditions to release extra operational flexibility for the management of reserve deliverability risk. The DRJCC is presented in (12).

$$\inf_{\mathbf{P} \in \mathbb{D}} \mathbf{P} \left\{ \begin{array}{l} \tau_{-j}^{NR/NS} \leq \tau_{j,t,s}^{NR/NS} \leq \bar{\tau}^{NR/NS}, \forall j, \\ \tau_{-i}^{IN} \leq \tau_{i,t,s}^{IN} \leq \bar{\tau}_i^{IN}, \forall i, \end{array} \right\} \geq 1 - \varepsilon \quad (12)$$

## 2.4 | Mathematical program with equilibrium constraints

By replacing the lower-level problem by its KKT conditions of the Lagrange equations, the bi-level problem can be converted into a single-level MPEC. The complete expression of the dual and complementarity slackness constraints can be found in Appendix A. Note that the appendix of this paper is attached online in [37]. Since market clearing prices for energy and reserve products are lower-level dual variables, there exist bilinear terms in the objective function of the bidding strategy (e.g.,  $\lambda_t^{R,U} R_{t,t}^U$ ). By applying the strong duality theory, the objective function can be reformulated in a linear form, which is presented in Appendix B.

## 3 | A DISTRIBUTIONALLY ROBUST L-SHAPED ALGORITHM BASED ON BILINEAR BENDER'S DECOMPOSITION

L-shaped algorithms (Bender's decomposition) are designed to tackle the two-stage distributionally robust programming. We revise the original distributionally robust L-shaped algorithm presented in [29] to deal with the proposed DRJCCP model developed in this paper. Given the day-ahead committed energy and reserve bids from the first stage, subproblems for each scenario is calculated and optimal cuts are generated to tighten the master problem. Then, the distribution separation problem is conducted to solve the expected real-time reschedule under the worst-case probability distribution. Overall steps are depicted in Figure 2.

### 3.1 | Compact form

In order to elaborate the proposed solution techniques in a reader-friendly way, the proposed DRJCCP model is abstracted in the compact form as in (13).

$$\min \mathbf{c}^T \mathbf{x} + v(\mathbf{x}) \quad (13a)$$

$$s.t. \mathbf{A}\mathbf{x} \leq \mathbf{b} \quad (13b)$$

where (13a) corresponds to the objective function in (1) with  $\mathbf{x}$  as the first-stage (bidding-related) decision variables. (13b) represents the constraints in (2) as well as the KKT conditions for the lower-level market clearing.  $v(\mathbf{x})$  denotes the second-stage objective function depicted in (1c), (1d), considering the worst realization of the probability distribution of the uncertainties.

The second-stage problem can be written as the following formulation in (14) using discrete scenario representation.

$$v(\mathbf{x}) = \max_{\pi_s \in \mathbb{D}} \sum_s \pi_s \mathbf{d}^T \mathbf{y}_s \quad (14a)$$

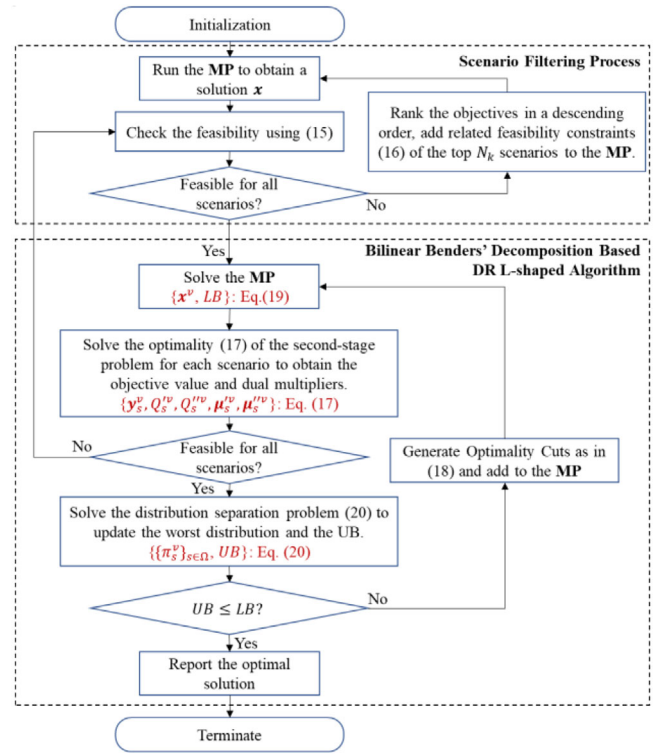


FIGURE 2 The schematic flowchart of the proposed algorithm.

$$s.t. \mathbf{C}\mathbf{x} + \mathbf{D}\mathbf{y}_s - \mathbf{f}_s \leq 0, \forall s \quad (14b)$$

$$(1 - \omega_s) (\mathbf{H}\mathbf{y}_s - \mathbf{g}_s) \leq 0, \forall s \quad (14c)$$

$$\lambda\theta + \sum_{s'} \hat{\pi}_{s'} v_{s'} \leq \varepsilon, \forall k \quad (14d)$$

$$\lambda \geq 0, \omega_s \in \{0, 1\}, \forall s \quad (14e)$$

$$\lambda\delta_{ss'} + v_{s'} - \omega_s \geq 0, \forall s, s' \in \mathcal{N} \quad (14f)$$

where  $\omega_s$  is a binary variable for indicating the responsive scenarios.  $\lambda, v_s$  are introduced dual variables.

Equation (14a) corresponds to the objective function in (1) and the second-stage constraints are rewritten explicitly using a bilinear formulation in (14b)–(14f). Equation (14b) represents the security constraints that should be satisfied under all occasions, corresponding to constraints (2)–(9). Equations (14d)–(14f) are introduced to equivalently represent the chance constraints in (12) [35]. Detailed proof is shown in Appendix C.  $\omega_s$  is a binary variable for indicating the responsive scenarios.  $\lambda, v_s$  are introduced dual variables. The bilinear constraint (14d) suggests that  $\mathbf{H}\mathbf{y}_s - \mathbf{g}_s \leq 0$  must be satisfied when  $\omega_s = 0$ . If  $\omega_s = 1$ , the scenario is selected as non-responsive scenario and the chance constraints do not need to be satisfied. The determination of  $\omega_s$  is restricted by (14e) and (14f).

### 3.2 | Scenario filtering method

By this reformulation in (14), the proposed model is converted to standard two-stage DRO model that can be solved by the distributionally robust L-shaped algorithm proposed in [29]. The application of this algorithm requires a relatively complete recourse for each scenario  $s$ . A straightforward method to achieve this requirement is to add operational constraints (14c), (14d) to the first-stage problem (13). However, this makes the size of the problem dramatically increase as more scenarios are included. We notice that only a small portion of the scenarios are extreme scenarios that most possibly violate the operational constraints. Here we propose a heuristic scenario filtering method (SFM) to deal with the issue. Main steps are presented as follows.

- Step 1. Initialize iteration counter  $l = 0$  an integer number  $N_k$ , critical scenario set  $\Pi^c = \{\emptyset\}$ . Run (13) to get an initial solution  $\mathbf{x}^0$ .
- Step 2. For each scenario  $s$ , run feasibility problem (15) and record the objective values  $F_s(\mathbf{x}^l)$ .

$$F_s(\mathbf{x}^l) = \min 1^T \boldsymbol{\sigma}'_s + 1^T \boldsymbol{\sigma}^{CC}_s \quad (15a)$$

$$\mathbf{D}\mathbf{y}_s \leq \mathbf{f}_s - \mathbf{C}\mathbf{x} + \boldsymbol{\sigma}'_s \quad (15b)$$

$$\mathbf{H}\mathbf{y}_s \leq \mathbf{g}_s + \boldsymbol{\sigma}^{CC}_s \quad (15c)$$

$$\mathbf{x} = \mathbf{x}^v : \boldsymbol{\omega}_s^v \quad (15d)$$

$$\boldsymbol{\sigma}^{CC}_s, \boldsymbol{\sigma}'_s \geq 0 \quad (15e)$$

Step 3. Rank the scenarios according to their objective values in the descending order. Choose the first  $N_k$  scenarios (denoted by  $s^{v1}, \dots, s^{vN_k}$ ) with non-zero objective values and add related constraints (16) as well as (14b) as feasibility cuts to the master problem. And then, update the critical scenario set  $\Pi^c \leftarrow \Pi^c \cup \{s^{v1}, \dots, s^{vN_k}\}$ . If added cuts in this iteration are non-empty, run (13) and update the first-stage solution  $\mathbf{x}^{v+1}$ , and let  $v = v + 1$ , go back to Step 2. If not, terminate the scenario filtering process.

Step 4. Return the feasibility constraints (16).

$$\mathbf{H}\mathbf{y}_s - \mathbf{g}_s \leq \mathbf{S}\boldsymbol{\omega}_s + \boldsymbol{\varphi}\boldsymbol{\omega}_s, \forall s \in \Pi^c \quad (16a)$$

$$\mathbf{S} = \mathbf{H}^+ \bar{\mathbf{y}}_s - \mathbf{H}^- \mathbf{y}_s - \mathbf{g}_s, \forall s \in \Pi^c \quad (16b)$$

$$\boldsymbol{\omega}_s = 0, \forall s \in \Pi \setminus \Pi^c \quad (16c)$$

### 3.3 | Bilinear benders' cut generation

As depicted in Figure 2, given the second-stage problem in (14) a mixed-integer linear program, the strong duality cannot be directly applied to generate valid cuts. On top of our bilinear

formulation, a bilinear variant of Benders' decomposition has been proposed in to efficiently solve chance constrained UC problems [23]. In this work, we adopt incorporate bilinear Benders' cuts into the L-shaped algorithm to deal with the proposed DRJCCP.

Given the first-stage solution  $\{\mathbf{x}^v, \boldsymbol{\omega}_s^v\}$ , the problem becomes separable in  $N$  scenarios with respect to the second stage variables  $\mathbf{y}$ . For each scenario  $s$ , the subproblem can be formulated as follows.

$$\mathcal{Q}_s(\mathbf{x}^v) = \min \mathbf{d}^T \mathbf{y}_s \quad (17a)$$

$$\mathbf{D}\mathbf{y}_s \leq \mathbf{f}_s - \mathbf{C}\mathbf{x}, \forall s \quad (17b)$$

$$(1 - \boldsymbol{\omega}_s^v) (\mathbf{H}\mathbf{y}_s - \mathbf{g}_s) \leq 0, \forall s \quad (17c)$$

$$\mathbf{x} = \mathbf{x}^v : \boldsymbol{\mu}_s^v \quad (17d)$$

where  $\boldsymbol{\mu}_s^v$  is the dual multipliers related to the first-stage solution.

If scenario  $s$  is chosen to be responsive (i.e.  $\boldsymbol{\omega}_s^v = 0$ ) in the  $v$ th-iteration of the first-stage solution, the optimality cuts in (18a) will be obtained and added to the master problem given optimal objective  $\mathcal{Q}_s^v$  and dual multipliers  $\boldsymbol{\mu}_s^{v'}$  for the constraints related to the first-stage solution. For the non-responsive scenario (i.e.  $\boldsymbol{\omega}_s^v = 1$ ), the optimal objective  $\mathcal{Q}_s^{v'}$  and dual variables  $\boldsymbol{\mu}_s^{v'}$  are calculated from the relaxed subproblem that neglects the chance constraints (17c), and then the related optimality cuts can be generated as in (18b). Note that the non-linear terms in (18) can be easily and equivalently reformulated to a tractable linear expression using McCormick Envelope [36]. These optimality cuts are valid only when the solution of  $\boldsymbol{\omega}_s$  remain consistent with  $\boldsymbol{\omega}_s^v$  in the following iterations.

$$\mathcal{Q}_s^{v'} (1 - \boldsymbol{\omega}_s) + \boldsymbol{\mu}_s^{v'T} (\mathbf{x} - \mathbf{x}^v) (1 - \boldsymbol{\omega}_s) \leq \theta_s, \forall s \quad (18a)$$

$$\mathcal{Q}_s^{v'} \boldsymbol{\omega}_s + \boldsymbol{\mu}_s^{v'T} (\mathbf{x} - \mathbf{x}^v) \boldsymbol{\omega}_s \leq \theta_s, \forall s \quad (18b)$$

Now we refer to the lower bound of the original problem (13) as the master problem (MP), defined as follows.

$$\min \mathbf{c}^T \mathbf{x} + \sum_s \pi_s^* \theta_s \quad (19a)$$

$$s.t. (13b), (16), (18) \quad (19b)$$

### 3.4 | Distribution separation problem

Given the optimal solutions of (19) and the confidence set in (11), the associated distribution separation problem is given by the following optimization model. In this case the worst probability distribution for all the scenarios can be calculated iteratively.

$$D^v = \max_{\pi_s, \mathbb{P} \in \mathbb{D}} \sum_s \pi_s (\mathcal{Q}_s^{v'} (1 - \boldsymbol{\omega}_s^v) + \mathcal{Q}_s^{v'} \boldsymbol{\omega}_s^v) \quad (20)$$

Then, the overall solution steps are depicted in Algorithm 1.



**ALGORITHM 1** Customized L-shaped method for DRJCCP

---

```

1: Initialization: Set iteration counter  $\nu = 0$ , scenario counter  $s = 1$  and a
   relative gap. Set the number for worst case selection  $N_k$ .  $UB = +\infty$ ,
    $LB = -\infty$  Run SFM method to get critical scenario set  $\Pi^c$  and add
   (16) to MP.
2: Solve MP to get  $x^0$ .
3: while  $UB > LB$  do
4:   for  $s \in \Omega$  do
5:     Solve the optimality problem (17);
6:     if infeasible then
7:        $\Pi^c \leftarrow \Pi^c \cup s$ , update related constraints (16) in MP.
8:     end if
9:     Obtain the objective values and derive dual multipliers  $\mu_s^v, \mu_s'^v$ .
10:  end for
11:  Solve the distribution separation problem (20) to get the  $\{\pi_s^v\}_{s \in \Omega}$ 
   using objective values  $Q_s^v, Q_s'^v$ .
12:  if  $UB > c^T x^v + \sum_s \pi_s^v (Q_s^v (1 - \omega_s^v) + Q_s'^v \omega_s^v)$  then
13:     $UB \leftarrow c^T x^v + \sum_s \pi_s^v (Q_s^v (1 - \omega_s^v) + Q_s'^v \omega_s^v)$ ;
14:    if  $UB \leq c^T x^v + \sum_s \pi_s^v (Q_s^v (1 - \omega_s^v) + Q_s'^v \omega_s^v)$  then
15:      Go to Line 23.
16:    end if
17:  end if
18:  Derive optimality cuts as in (18), add to the master problem MP.
19:  Solve the master problem MP;
20:   $\{x^v, \omega_s^v\} \leftarrow$  optimal solution of MP and  $LB \leftarrow$  optimal objective
   value of MP
21:  Set  $\nu \leftarrow \nu + 1$ ;
22: end while
23: return optimal solution  $x^v$  and objective value  $UB$ .

```

---

We can extend the proof in [29] to deduce that this structure is able to solve the proposed DRJCCP in finitely many iterations.

## 4 | CASE STUDY

### 4.1 | Test system setup and basic results

In this section, numerical tests are carried out on an IEHS-ISO5 bus system to validate the performance of the proposed model. The IEHS test system consists of a 15-bus-PDN system and a 10-node-DHN system. Also, a modified PJM-5 bus transmission system is incorporated for simulation of the transmission constrained market clearing. We consider a 15-bus power distribution system (PDN-15) with 5.04 MW peak power load integrated with 10-node district heating system (DHN-10) with 2.27 MW peak heating load, which is located at bus 2 of the ISO-5 bus system. Two CHP units, one non-CHP thermal unit, two electric boilers, two PV panels are presented in the integrated system. Based on the historic data from a district in China, 100 representative scenarios are generated by k-means method to conduct the optimization. The confidence level  $1 - \varepsilon$  for chance

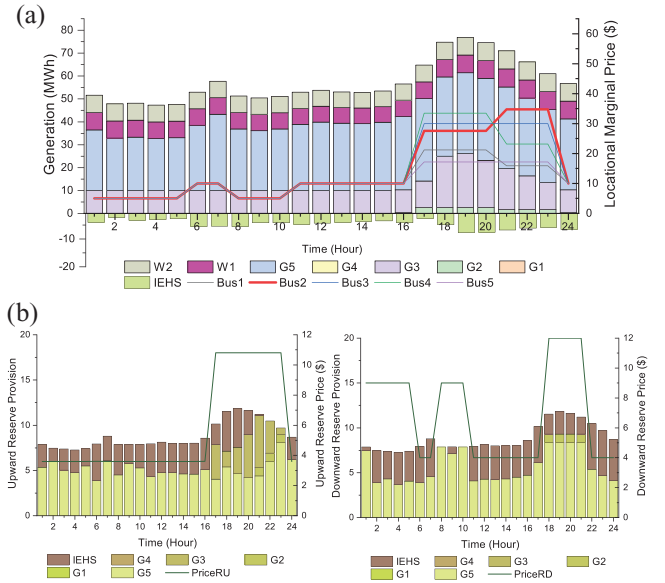


**FIGURE 3** Clearing results of ISO energy: (a,b) reserve markets.

constraints is set to 95%. And the ratio of maximal deviation  $\delta$  is set to 5%.

In our test, 100 clustered scenarios assigned with the occurrence probabilities are utilized to model the uncertainty of the reserve deployment ratio as well as the RES output fluctuation. The power load profiles in both IEHS and the whole ISO power system valley around 1–6 hour and peak around 17–22 hour during a day. This causes a relatively large fluctuation in the energy prices in the ISO market, ranges from as low at \$5/MWh to as high as \$37.23/MWh, particularly, for some congested nodes. The results for the ISO energy and reserve clearing are shown in Figure 3.

### 4.2 | The value of virtual thermal energy storage

Here, the DHN works as a virtual energy storage system so that real-time power deviations can be balanced through power-heat coordination. To quantify the effect of different modelling techniques of thermal networks on the performance of the bidding strategy, we generate four cases as presented below:

Case 0 (Fixed thermal load model): The heat scheduling is pre-optimized such that the DHN is modelled as a fixed thermal load.

Case 1 (Energy-only model): Temperature profiles are neglected, while only the supply-demand balance is considered.

Case 2 (simplified network model): The temperature change along the pipeline is considered while the time delays and energy storage characteristics are ignored (This model is most commonly used in the IEHS operation.)

Case 3 (Detailed network model): Detailed thermal flow model with pipeline storage representation is adopted.

To assess the effectiveness of these models, we utilize the detailed thermal network model applied in Case 3 to verify the

**TABLE 1** Impact of different thermal network models.

Case	Total cost/\$	Day-ahead operating cost/\$		Real time cost/\$	Actual total cost/\$
		Energy	Reserve		
Case 0	1808.43	1820.59	-509.59	497.43	1891.41
Case 1	1502.49	1719.46	-705.56	515.11	Infeasible
Case 2	1573.47	1689.73	-600.28	484.02	1557.18
Case 3	1520.45	1732.55	-665.79	453.68	1520.45

actual performance of all these cases. The comparison results of the four cases are reported in Table 1. The fixed load model in Case 0 is obviously the least profitable one. Since the heat scheduling is predefined, no flexibility can be provided from the heat system side. Case 1 looks like to achieve the optimal total cost. However, the solution is derived based on the energy-only model without considering temperature profiles and the network topology. This simplification overestimates the flexibility and causing feasibility issue in the real-time operation. Case 2 neglects the pipeline storage characteristic, which limits the reserve provision capability of the IEHS. Case 3, utilizing the detailed thermal network model, fully capitalizes on the operational flexibility of the DHN, thereby benefiting the integrated system as a whole.

### 4.3 | Reserve deliverability risk management

Based on Case 3, six cases are designed to study the impact of different risk management models:

Case 3.0 (Deterministic model): The basic model refers to the day-ahead bidding optimization model, where the forecast of uncertainty sources is assumed to be accurate.

Case 3.1 (Traditional SP model): It is assumed that the probability distribution of uncertainties is known.

Case 3.2 (Traditional RO model): Only the worst-case scenarios are considered to provide a rather conservative solution that ensures the reserve deliverability under any situation.

Case 3.3 (DRO model): Traditional DRO model is adopted given an ambiguity set for the probability distribution of uncertainties.

Case 3.4 (CCP model): Based on the Case 3.1, chance constraints are considered.

Case 3.5 (DRJCC model): Our proposed model combines the joint chance constraints into DRO model to optimally choose non-responsive scenarios to neglect for better economic performance.

To visualize the committed reserve provision of the IEHS, the committed operational flexibility under the six cases is presented in Figure 4a–f, respectively. In this figure, “P” represents the day-ahead committed energy bid of IEHS, while “P+RD” and “P-RU” are upper and lower bounds of the real-time net load profiles of IEHS considering committed up/downward reserve capacities. We use these bounds to illustrate the committed flexibility of the IEHS. Monte Carlo method is then

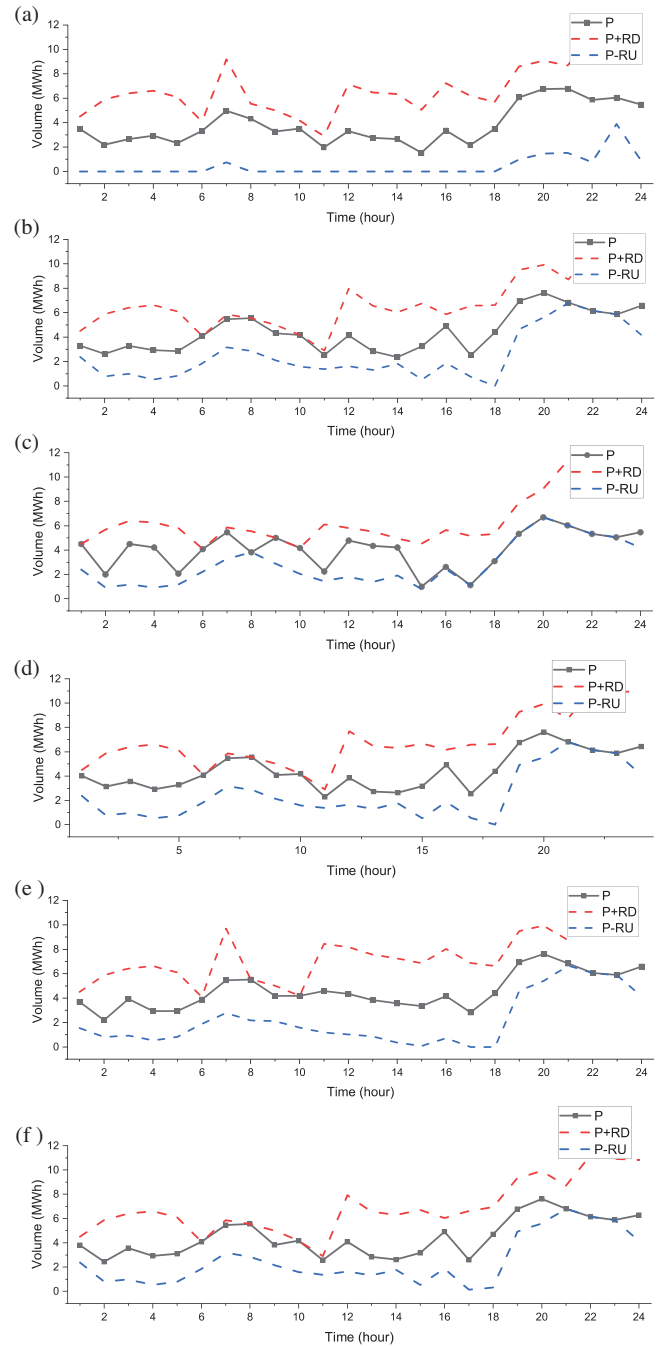


**FIGURE 4** Power and reserve schedule under different cases: (a) deterministic model; (b) stochastic programming (SP) model; (c) robust optimization (RO) model; (d) distributionally robust optimization (DRO) model; (e) chance constrained programming (CCP) model; (f) distributionally robust joint chance constrained (DRJCC) model.

employed to generate 1000 scenarios to estimate the out-of-sample performance of these cases. Results of the six cases are summarized in Table 2, and the detailed analyses are presented as follows.

Case 3.0: The deterministic model utilizes an averaged scenario to optimize the optimal bidding strategy. As shown in Figure 4a, the operator commits the largest area for reserve provision. Since uncertainties are ignored, as depicted in Table 2,

**TABLE 2** Reserve deliverability risk and profitability test.

Case	Total operating costs/\$		Number of non-responsive scenarios
	In-sample	Out-of-sample	
Case 3.0: Deterministic	1219.92	Infeasible	Infeasible
Case 3.1: SP	1542.56	1611.40	0
Case 3.2: RO	1709.36	1716.81	0
Case 3.3: DRO	1559.43	1590.60	0
Case 3.4: CCP	1480.39	1547.24	67/1000
Case 3.5: DRJCCP	1520.45	1561.70	14/1000

Abbreviations: SP, stochastic programming; RO, robust optimization; DRO, distributionally robust optimization; CCP, chance constrained programming; DRJCCP, distributionally robust joint chance constrained.

this model provides a least-cost solution (\$1219.92) based on accurate forecast on uncertainty sources, which is way better than other cases. This result, however, is overly-optimistic and strongly relies on the forecast so that it fails to pass the out-of-sample test because the reserve deliverability requirement cannot be satisfied.

Case 3.1: By applying the SP method, the generated 1000 scenarios are assigned with a given probability. This yields a relatively expensive but reliable solution at \$1542.56 compared to Case 3.0. However, the true distribution could deviate from the empirical one, resulting in a considerable increase of the operating cost (+\$68.54) in the out-of-sample performance.

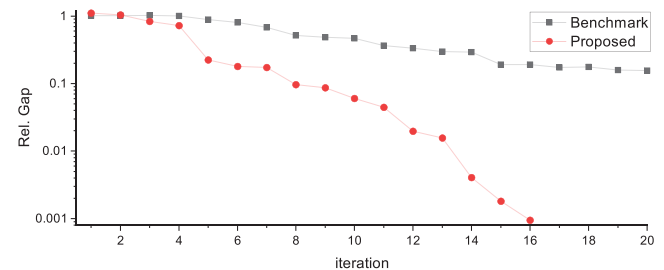
Case 3.2: Utilizing the RO method, this case provides a rather conservative solution that under any possible realization of the uncertainties. As such, the day-ahead committed reserve is very limited as in Figure 4c. Although the out-of-sample cost is close to the in-sample cost, the result is the least economic at \$1809.36, which is usually unacceptable in practice for a profit-pursuing operator.

Case 3.3: The application of the DRO method provide an intermediate solution between Case 3.1 and Case 3.2. Compared to the SP method, though with a slightly higher in-sample optimized cost (+\$16.87), it derives a better out-of-sample performance by considering the worst probability distribution. And it is less conservative compared to the RO method (−\$249.93) and more beneficial to the operator.

Case 3.4: The above cases do not consider the flexibility of thermal supply quality. In this case, chance constraints on temperature-related constraints are introduced to the SP method in Case 3.1 to yield a stochastic chance constrained model. This model greatly increases the capability of reserve provision of the IEHS and offers the most profitable solution among all these cases in both in-sample and out-of-sample tests (\$1480.39/\$1547.24). However, chance constraints are restricted by a confidence level  $\varepsilon$  that indicates the maximal proportion of non-responsive scenarios allowed. That is, only in these selected scenarios, the quality of thermal energy supply can be degraded. In the out-of-sample test, 67 out of 1000 scenarios are chosen to be non-responsive in order to guarantee the reserve deliverability, which is higher than the setup of the confidence level ( $6.7\% \geq 5\%$ ). Because of uncertain in

**TABLE 3** Computation performance of the proposed algorithm.

Number of scenarios	Case	Relative Gap	Time/s
20	Proposed	0.06%	324.82
	Benchmark	0.07%	372.73
50	Proposed	0.08%	372.34
	Benchmark	0.08%	439.64
100	Proposed	0.09%	1224.30
	Benchmark	0.20%	9579.83

**FIGURE 5** Gap between upper and lower bounds of the objective value.

the true probability distribution, the confident level of chance constraints in CCP cannot be guaranteed.

Case 3.5: Taking the advantages of CCP and DRO, the DRJCCP is adopted in this case, generating a solution with a better tradeoff between robustness and effectiveness. To ensure the reserve deliverability under the worst probability distribution, the committed reserve capacity is relatively conservative compared to Case 3.4. The optimized cost is \$1520.45, with a relatively good out-of-sample performance at \$1561.70. Besides, only 14 out of 1000 scenarios ( $1.4\% \leq 5\%$ ) provide low-quality heat in exchange of the satisfaction of reserve deliverability.

#### 4.4 | Computation efficiency improvement

In order to model the characteristics of the uncertainty factors, the proposed DRJCC programming should involve a large number of scenarios, which can cause intractability due to the significant computation burden. The paper introduces a scenario filtering method (SFM) and efficiently bilinear benders decomposition method to solve this problem. Due to the non-convexity of the DRJCCP, the proposed model cannot be solved directly via commercial solvers. This class of problem can be solved by the distributionally robust L-shaped algorithm presented in [29]. To analyse the effectiveness of our modified algorithm, we solved this model using our customized L-shaped algorithm, referred to as “Proposed”, as well as a traditional L-shaped algorithm, referred to as “Benchmark”. The related results are presented in Table 3. We can more directly see the changes of the gaps between the upper bound and lower bound in the case with 100 scenarios in Figure 5. In this figure, the

**TABLE 4** Scalability test on the PDN-123-DHN-32 test system.

Number of scenarios	Objective/\$	Computation time/s	
		Proposed	Benchmark
50	2962.4	1024.88	1326.29
100	2946.2	1693.73	3884.64
250	2972.8	3930.61	Out-of-memory
500	2981.9	9402.98	Out-of-memory

proposed algorithm converges to the stop criteria (relative gap smaller than  $1e-3$ ) in 15 iterations. However, in the benchmark case, the convergence is way slower. In the 20th iteration, the benchmark case is still far from the stop criteria. This indicates the efficiency of the proposed algorithm in computation.

#### 4.5 | Scalability analysis

To assess the scalability of our proposed model, we conducted tests on a large-scale IEHS system, which consists of a modified IEEE 123-bus PDN and a 32-node DHN with varying numbers of scenarios. The results of these tests are summarized in Table 4. We observed that the computation time increased nearly linearly with the number of scenarios using the proposed algorithm. On the other hand, the benchmark algorithm demonstrated good performance when the scenario set was small. However, as the number of scenarios increased, the computation burden grew dramatically, eventually leading to an out-of-memory issue with 250 scenarios. When the number of scenarios reaches 500, the computation time via the proposed algorithm is 9402.98 s, which is still acceptable as a day-ahead optimization problem. These findings highlight the efficiency and practicality of our proposed model and algorithm as a day-ahead scheduling optimization solution. We should also note that problem can be solved parallelly, which can further reduce the computation time.

### 5 | CONCLUSION

This paper presents a two-stage distributionally robust strategic participation framework of the IEHS in day-ahead energy and reserve markets. Specifically, we present a novel reserve provision model for the IEHS that accounts for its energy-limited nature and realistically illustrates its ability to provide reserve under diverse uncertainties. Then, to provide a risk-averse bidding strategy of the IEHS, we employ a DRO framework to evaluate the deliverability risks. Distributionally joint chance constraints are incorporated to relax temperature constraints of DHN and avoid uninstructed deviation penalties in extreme scenarios. We prove that these constraints are equivalent to a set of mixed integer inequalities so that the proposed model can be converted into a tractable formulation. To effectively solve this problem, a customized L-shaped algorithm with scenario

filtering method is proposed to improve computation efficiency. Numerical results show that (i) incorporating the detailed thermal flow model enhances the flexibility of the IEHS in reserve provision. (ii) Compared to other risk management models, the proposed DRJCC model can provide a reliable and beneficial bidding strategy for a risk-averse IEHS operator. (iii) Computation tests show that the proposed algorithm is efficient and the DRJCC model is scalable. Future work could explore the extension of the proposed framework to decentralized operational structures.

### NOMENCLATURE

$\bar{P}_{fl}$	Capacity of line $fl$ in the transmission system
$P_{-l}^{GC}, \bar{P}_l^{GC}$	Upper/lower bounds of the generator companies at bus $l$
$\frac{-E}{\theta_l} / RU / RD$	Price caps for the energy and reserve markets
$\hat{p}_{n,t}^D / \hat{b}_{i,t}^D$	power/thermal load at bus $n$ /node $i$
$\tilde{\lambda}_{l,t,s}^E$	Real-time LMP at bus $l$
$\hat{\pi}_s$	Probability of scenario $s$ in empirical distribution $\hat{\mathbf{P}}$
$\tau^{S/R} / \bar{\tau}^{S/R}$	Lower/upper bounds of for supply/return network temperature
$\hat{\tau}^{AM}$	Ambient temperature
$b_{g,t,s}^{CHP/EB}$	Heat generation of the DER $g$ at time $t$ of scenario $s$
$N^{HS/HD}$	Set of source/demand nodes in the DHN
$J_{ij,t}$	The thermal loss coefficient of supply/return pipeline $ij$ at time $t$
$K_{ij,t,k}$	Coefficient defining the outlet temperature of pipeline $ij$ at time $t$ by the input at time $k$
$P_{mn,t,s} / Q_{mn,t,s}$	Active/reactive power flow of distribution line $mn$
$P_{t,s}^{PCC,D}$	Real-time power deviation of IEHS at time $t$ of scenario $s$
$P_{t,s}^{mis}$	Real-time reserve request mismatch at time $t$ of scenario $s$
$R_{l,t}^{GC/EH,U/D}$	Cleared quantity for up/down-ward reserve of the generator company/the IEHS
$R_t^{Sys,U/D}$	Systematic requirements for up/down reserves
$U_i, \eta^H$	Heat conductance of building at node $i$ , Heat capacity of the consumers (buildings)
$\bar{V} / \bar{V}$	Lower/upper bound of voltage
$\bar{c}_w, \rho_w$	Specific heat capacity, density of water
$m_{ij,t}$	Mass flow rate of pipeline $ij$ at time $t$
$\theta_{l,t}^{EH,E} / RU / RD$	Bid prices of the IEHS for ISO energy, upward/downward reserve market
$\theta_{l,t}^{GC}, \theta_{l,t}^{GC,RU/RD}$	Price bids of generator company located at bus $l$ for energy and up/down-ward reserves
$\hat{p}_{g,t,s}^{CHP/TU/EB/RE}$	Power generation of the DER $g$ at time $t$ of scenario $s$



$p_{l,t}^D$	Load at bus $l$ in the transmission system
$p_{l,t}^{EH,Bid}$	Bid quantities of the IEHS
$p_{l,t}^{GC,Bid}$	Bid quantity of the generator company at bus $l$
$p_{l,t}^{GC/EH}$	Cleared quantity for power of the generator company/the IEHS located at bus $l$
$p_{n,t}^D/b_{i,t}^D$	power/thermal energy at bus $n$ /node $i$ consumed via networks
$r_{mn}, x_{mn}$	Resistance and reactance of power line
$r_{l,s}^R$	Real-time reserve request from the ISO
$v_{m,t,s}$	Voltage magnitude at bus $m$ of the IEHS
$N_j^{R(+)} / N_j^{R(-)}$	Set of ending/starting nodes of pipelines with starting/ending node $j$ in return networks
$N_j^{S(+)} / N_j^{S(-)}$	Set of ending/starting nodes of pipelines with starting/ending node $j$ in supply networks
$N_n^{pr} / N_n^{ch}$	Set of parent/children buses of bus $n$
$\alpha_{l,s}^{R,U/D}$	Deployed ratio for upward/downward reserve
$\eta_g^{P2H}$	Power-to-heat ratio of co-generator $g$
$\lambda_{l,t}^E, \lambda_{l,t}^{RU/RD}$	Locational marginal price (LMP), up/downward reserve prices of bus $l$ at time $t$
$\lambda_t^{pen}$	Uninstructed deviation penalty of the reserve deployment
$\pi_{s,s,t}$	Probability in joint distribution $\mathbf{Q}$
$\pi_s$	Probability of scenario $s$ in true distribution $\mathbf{P}$
$\tau_{i,t,s}^{GS/GR/DS/DR}$	Temperature at generation (G)/demand (R) node $i$ of the supply (SN)/return network (RN)
$\tau_{i,t,s}^{IN}, p_{n,t,s}^{E2H}$	Indoor temperature of the demand user at node $i$ , power output of the power-to-heat devices
$\tau_{i,t,s}^{NS/R}$	Mixed temperature at the node $i$ of the SN/RN
$\tau_{ij,t,s}^{S/R,in/out}$	Temperatur at the inlet/outlet of the pipeline $ij$ of the SN/RN
$\Xi(i)$	Index of coupling DHN node of bus $i$ in PDN
$g/G^k$	Index/set of distributed energy resources (DER), $k = \{CHP, EB, TU, RE\}$
$i, j, k / N^H$	Index/set of nodes in the DHN
$l, f / N^{TS}$	Index/set of buses in the transmission system
$m, n, b / N^E$	Index/set of buses in the PDN
$s$	Index of scenarios
$t / T$	Index/set of time periods
$\beta$	Ratio of maximal reactive power
$\delta$	Ratio of maximal deviation from reserve request
$\varepsilon$	Confidence level for chance constraints
$\theta$	Tolerance level for the Wasserstein distance between empirical and true distribution
$\epsilon, L$	Heat conductance, length of pipeline

## AUTHOR CONTRIBUTIONS

Yang Chen: Conceptualization; Methodology; Writing—original draft. Jianxue Wang: Software; Supervision; Writing—review and editing. Siyuan Wang: Methodology; Resources; Writing—review and editing. Rui Bo: Supervision; Validation. Chenjia Gu: Data curation; Writing—review and editing. Qingtao Li: Resources; Validation.

## ACKNOWLEDGEMENTS

This work was supported by the Natural Science Foundation of Jiangsu Province “Research on Frontier Basic Theory and Method of Security Defense for Power Systems with High-dimensional Uncertain Factors” (No. BK20222003).

## CONFLICT OF INTEREST STATEMENT

The authors declare no conflicts of interest.

## DATA AVAILABILITY STATEMENT

The data that support the findings of this study are available from the corresponding author upon reasonable request.

## ORCID

Jianxue Wang  <https://orcid.org/0000-0002-0596-0815>

Siyuan Wang  <https://orcid.org/0000-0003-1443-0709>

Chenjia Gu  <https://orcid.org/0000-0002-9551-7250>

## REFERENCES

- Lu, Y., Wen, Y., Wang, Y., Li, T., Tang, Q., Xu, W.: Clean generation mix transition: Large-scale displacement of fossil fuel-fired units to cut emissions. *IEEE Ind. Appl. Mag.* 28(2), 14–26 (2022). <https://doi.org/10.1109/MIAS.2021.3065330>
- Mancarella, P.: MES (multi-energy systems): An overview of concepts and evaluation models. *Energy*. 65, 1–17 (2014). <https://doi.org/10.1016/j.energy.2013.10.041>
- Chen, X., et al.: Increasing the flexibility of combined heat and power for wind power integration in China: Modeling and implications. *IEEE Trans. Power Syst.* 30(4), 1848–1857 (2015). <https://doi.org/10.1109/TPWRS.2014.2356723>
- Guelpa, E., Bisch, A., Verda, V., Chertkov, M., Lund, H.: Towards future infrastructures for sustainable multi-energy systems: A review. *Energy*. 184, 2–21 (2019). <https://doi.org/10.1016/j.energy.2019.05.057>
- Khatibi, M., Bendtsen, J.D., Stoustrup, J., Molbak, T.: Exploiting power-to-heat assets in district heating networks to regulate electric power network. *IEEE Trans. Smart Grid*. 12(3), 2048–2059 (2021). <https://doi.org/10.1109/TSG.2020.3044348>
- Sharifi, R., Fathi, S.H., Vahidinasab, V.: A review on Demand-side tools in electricity market. *Renewable Sustainable Energy Rev.* 72, 565–572 (2017). <https://doi.org/10.1016/j.rser.2017.01.020>
- Marnieris, I.G., et al.: Optimal participation of RES aggregators in energy and ancillary services markets. *IEEE Trans Ind Appl.* 59, 232–243 (2022). <https://doi.org/10.1109/TIA.2022.3204863>
- Di Somma, M., Graditi, G., Siano, P.: Optimal bidding strategy for a DER aggregator in the day-ahead market in the presence of demand flexibility. *IEEE Trans. Ind. Electron.* 66(2), 1509–1519 (2019). <https://doi.org/10.1109/TIE.2018.2829677>
- Ghadi, M.J., Ghavidel, S., Rajabi, A., Azizivahed, A., Li, L., Zhang, J.: A review on economic and technical operation of active distribution systems. *Renewable Sustainable Energy Rev.* 104, 38–53 (2019). <https://doi.org/10.1016/j.rser.2019.01.010>
- Kong, X., Yong, C., Wang, C., Chen, Y., Yu, L.: Optimal strategy of active distribution network considering source–network–load. *IET Gener. Transm. Distrib.* 13(24), 5586–5596 (2019). <https://doi.org/10.1049/iet-gtd.2018.5781>

11. Ravi, A., Bai, L., Cecchi, V., Ding, F.: Stochastic strategic participation of active distribution networks with high-penetration DERs in wholesale electricity markets. *IEEE Trans. Smart Grid.* 14(2), 1515–1527 (2022). <https://doi.org/10.1109/TSG.2022.3196682>
12. Mohammadi, M., Noorollahi, Y., Mohammadi-ivatloo, B., Yousefi, H.: Energy hub: From a model to a concept – A review. *Renewable Sustainable Energy Rev.* 80, 1512–1527 (2017). <https://doi.org/10.1016/j.rser.2017.07.030>
13. Oskoue, M.Z., Mohammadi-ivatloo, B., Abapour, M., Shafiee, M., Anvari-Moghaddam, A.: Strategic operation of a virtual energy hub with the provision of advanced ancillary services in industrial parks. *IEEE Trans. Sustainable Energy.* 12(4), 2062–2073 (2021). <https://doi.org/10.1109/TSTE.2021.3079256>
14. Li, R., Wei, W., Mei, S., Hu, Q., Wu, Q.: Participation of an energy hub in electricity and heat distribution markets: An MPEC approach. *IEEE Trans. Smart Grid.* 10(4), 3641–3653 (2019). <https://doi.org/10.1109/TSG.2018.2833279>
15. Li, Z., Wu, W., Shahidehpour, M., Wang, J., Zhang, B.: Combined heat and power dispatch considering pipeline energy storage of district heating network. *IEEE Trans. Sustainable Energy.* 7(1), 12–22 (2016). <https://doi.org/10.1109/TSTE.2015.2467383>
16. Zhang, M., et al.: Day-ahead stochastic scheduling of integrated electricity and heat system considering reserve provision by large-scale heat pumps. *Appl. Energy.* 307, 118143 (2022). <https://doi.org/10.1016/j.apenergy.2021.118143>
17. Tang, Z., Liu, Y., Wu, L., Liu, J., Gao, H.: Reserve model of energy storage in day-ahead joint energy and reserve markets: A stochastic UC solution. *IEEE Trans. Smart Grid.* 12(1), 372–382 (2021). <https://doi.org/10.1109/TSG.2020.3009114>
18. Liu, Y., Wu, L., Yang, Y., Chen, Y., Baldick, R., Bo, R.: Secured reserve scheduling of pumped-storage hydropower plants in ISO day-ahead market. *IEEE Trans. Power Syst.* 36(6), 5722–5733 (2021). <https://doi.org/10.1109/TPWRS.2021.3077588>
19. Zhou, Y., Shahidehpour, M., Wei, Z., Li, Z., Sun, G., Chen, S.: Distributionally robust co-optimization of energy and reserve for combined distribution networks of power and district heating. *IEEE Trans. Power Syst.* 35(3), 2388–2398 (2020). <https://doi.org/10.1109/TPWRS.2019.2954710>
20. Khalili, T., Ganjehlou, H.G., Bidram, A., Nojavan, S., Asadi, S.: Financial risk-based scheduling of micro grids accompanied by surveying the influence of the demand response program. In: *Conference Record - Industrial and Commercial Power Systems Technical Conference.* Las Vegas, NV (2021). <https://doi.org/10.1109/ICPS51807.2021.9416627>
21. Mehdi pourpicha, H., Wang, S., Bo, R.: Developing robust bidding strategy for virtual bidders in day-ahead electricity markets. *IEEE Open Access J. Power Energy.* 8, 329–340 (2021). <https://doi.org/10.1109/OAJPE.2021.3105097>
22. Zhao, T., Pan, X., Yao, S., Ju, C., Li, L.: Strategic bidding of hybrid AC/DC microgrid embedded energy hubs: A two-stage chance constrained stochastic programming approach. *IEEE Trans. Sustainable Energy.* 11(1), 116–125 (2020). <https://doi.org/10.1109/TSTE.2018.2884997>
23. Zhang, Y., Wang, J., Zeng, B., Hu, Z.: Chance-constrained two-stage unit commitment under uncertain load and wind power output using bilinear benders decomposition. *IEEE Trans. Power Syst.* 32(5), 3637–3647 (2017). <https://doi.org/10.1109/TPWRS.2017.2655078>
24. Heris, M.N., et al.: Evaluation of hydrogen storage technology in risk-constrained stochastic scheduling of multi-carrier energy systems considering power, gas and heating network constraints. *Int. J. Hydrogen Energy.* 45(55), 30129–30141 (2020). <https://doi.org/10.1016/j.ijhydene.2020.08.090>
25. Daneshvar, M., Mohammadi-ivatloo, B., Zare, K., Asadi, S., Anvari-Moghaddam, A.: A novel operational model for interconnected microgrids participation in transactive energy market: A hybrid IGDT/stochastic approach. *IEEE Trans. Ind. Inf.* 17(6), 4025–4035 (2021). <https://doi.org/10.1109/TII.2020.3012446>
26. Wang, S., Zhao, C., Fan, L., Bo, R.: Distributionally robust unit commitment with flexible generation resources considering renewable energy uncertainty. *IEEE Trans. Power Syst.* 37(6), 4179–4190 (2022). <https://doi.org/10.1109/TPWRS.2022.3149506>
27. Rayati, M., Bozorg, M., Cherkaoui, R., Carpita, M.: Distributionally robust chance constrained optimization for providing flexibility in an active distribution network. *IEEE Trans. Smart Grid.* 13(4), 2920–2934 (2022). <https://doi.org/10.1109/TSG.2022.3154023>
28. Zhou, Y., Shahidehpour, M., Wei, Z., Li, Z., Sun, G., Chen, S.: Distributionally robust unit commitment in coordinated electricity and district heating networks. *IEEE Trans. Power Syst.* 35(3), 2155–2166 (2020). <https://doi.org/10.1109/TPWRS.2019.2950987>
29. Bansal, M., Huang, K.-L., Mehrotra, S.: Decomposition algorithms for two-stage distributionally robust mixed binary programs. *SIAM J. Optim.* 28(3), 2360–2383 (2018). <https://doi.org/10.1137/17M1115046>
30. Ji, R., Lejeune, M.A.: Data-driven distributionally robust chance-constrained optimization with Wasserstein metric. *J. Global Optim.* 79(4), 779–811 (2021). <https://doi.org/10.1007/s10898-020-00966-0>
31. Yang, J., et al.: A penalty scheme for mitigating uninstructed deviation of generation outputs from variable renewables in a distribution market. *IEEE Trans. Smart Grid.* 11(5), 4056–4069 (2020). <https://doi.org/10.1109/TSG.2020.2993049>
32. Cao, X., Wang, J., Wang, J., Zeng, B.: A risk-averse conic model for networked microgrids planning with reconfiguration and reorganizations. *IEEE Trans. Smart Grid.* 11(1), 696–709 (2020). <https://doi.org/10.1109/TSG.2019.2927833>
33. Li, Z., Wu, L., Xu, Y.: Risk-averse coordinated operation of a multi-energy microgrid considering voltage/var control and thermal flow: An adaptive stochastic approach. *IEEE Trans. Smart Grid.* 12(5), 3914–3927 (2021). <https://doi.org/10.1109/TSG.2021.3080312>
34. Zhao, H., Wang, B., Pan, Z., Sun, H., Guo, Q., Xue, Y.: Aggregating additional flexibility from quick-start devices for multi-energy virtual power plants. *IEEE Trans. Sustainable Energy.* 12(1), 646–658 (2021). <https://doi.org/10.1109/TSTE.2020.3014959>
35. Ji, R., Lejeune, M.A.: Data-driven distributionally robust chance-constrained optimization with Wasserstein metric. <https://ssrn.com/abstract=3201356>
36. Bergamini, M.L., Aguirre, P., Grossmann, I.: Logic-based outer approximation for globally optimal synthesis of process networks. *Comput. Chem. Eng.* 29(9), 1914–1933 (2005). <https://doi.org/10.1016/j.compchemeng.2005.04.003>
37. Chen, Y., et al.: Appendix. [Online]. Available: [https://drive.google.com/drive/folders/1rsz\\_UkSt417TagZXxH4oDzfD-4W4C\\_q?usp=sharing](https://drive.google.com/drive/folders/1rsz_UkSt417TagZXxH4oDzfD-4W4C_q?usp=sharing) (2023). Accessed 20 June 2023

**How to cite this article:** Chen, Y., Wang, J., Wang, S., Bo, R., Gu, C., Li, Q.: Managing reserve deliverability risk of integrated electricity-heat systems in day-ahead market: A distributionally robust joint chance constrained approach. *IET Gener. Transm. Distrib.* 1–14 (2023). <https://doi.org/10.1049/gtd2.12907>